# CONTAMINATED MULTIBAND SIGNAL IDENTIFICATION VIA DEEP LEARNING

*Youye Xie, Michael B. Wakin, and Gongguo Tang*

Department of Electrical Engineering, Colorado School of Mines, Golden, CO, USA

2021 IEEE Statistical Signal Processing Workshop (SSP) | 978-1-7281-5767-2/21/$31.00 ©2021 IEEE | DOI: 10.1109/SSP49050.2021.9513845

## ABSTRACT

Multiband signals, whose active frequencies lie within continuous intervals, arise in a wide range of applications like radar imaging. In this paper, given limited and varying-length time-domain samples of a contaminated multiband signal, we propose novel deep networks to estimate the number of bands and locate the bands' centers. A multiband signal representation model, which combines the long short-term memory (LSTM) and convolutional neural network, is trained to map varying-length observed samples to a frequency spectrum representation. A counting model then counts the number of bands based on the estimated spectrum. Combining the spectrum representation and estimated number of bands, the bands' centers can be recovered efficiently and automatically. Numerical experiments demonstrate that the proposed method is very effective and can leverage extended samples for better performance. Moreover, it outperforms other deep architectures for line spectral estimation at different noise levels and is much faster than an atomic norm-based method.

***Index Terms***— multiband signal, deep learning, super resolution, signal decomposition

## 1. INTRODUCTION

### 1.1. Contaminated Multiband Signal Identification

Conventional line spectral estimation [1] appears widely in many applications, e.g., power electronics [2]. Mathematically, one observes a time-domain *multitone* signal

$$y(t) = \sum_{j=1}^{M} A_j e^{i2\pi F_j t} + \eta(t) \tag{1}$$

where the number of tones $M$ is unknown, $A_j \in \mathbf{C}$ is a complex weight consisting of the unknown amplitude and phase, $F_j$ is the unknown frequency of interest, and $\eta(t)$ denotes additive Gaussian noise. In [3, 4], deep networks are proposed that solve the line spectral estimation problem with competitive performance. These networks give insight into the connections between a fundamental problem in signal processing and an emerging tool in machine learning.

The *multiband* signal identification problem generalizes the model in (1), such that each component is supported over a continuous narrow band in the frequency domain. Namely, $y(t)$ has its continuous-time Fourier transform, $Y(F)$, supported on a union of several bands,

$$\mathcal{F} = \bigcup_{j=1}^{M} [F_j - B_j, F_j + B_j], \quad y(t) = \int_{\mathcal{F}} Y(F) e^{i2\pi F t} dF + \eta(t). \tag{2}$$

This work was supported by NSF grant CCF–1704204. Email: {youyexie, mwakin, gtang}@mines.edu

Here $B_j$ is the width of the band whose center is $F_j$. Such multiband signals arise in applications like radar imaging [5] and communication [6]. Unfortunately, the deep networks in [3, 4] are not designed to accommodate multiband signals. In addition, most deep architectures [3, 4, 7, 8] for signal processing problems only allow a fixed-length input signal, while leveraging extended samples for better identification accuracy is characteristic of many signal processing techniques like the discrete Fourier transform (DFT).

In this paper, we propose novel deep networks to tackle the multiband signal identification problem while allowing for input signals of different lengths. After uniform and non-aliased sampling with sampling interval $T_s$, the multiband signal has the form [9–11]

$$\boldsymbol{y} = \sum_{j=1}^{M} A_j \boldsymbol{a}(f_j) \odot \int_{-W_j}^{W_j} \boldsymbol{a}(f) m_j(f) df + \boldsymbol{\eta} \in \mathbf{C}^N \tag{3}$$

where $\boldsymbol{a}(f) = [e^{i2\pi f 0}, e^{i2\pi f 1}, \cdots, e^{i2\pi f(N-1)}]^T$, $N$ is the length of the observed samples, $f_j = T_s F_j \in [-0.5, 0.5)$ denotes the band's digital frequency center, $W_j = T_s B_j \neq 0$ denotes the digital band width, and $m_j(f)$ is the envelope of the $j$-th band in the digital frequency domain. Moreover, $(.)^T$ denotes the transpose operator and $\odot$ denotes the element-wise (Hadamard) product.

Given only the sampled signal vector $\boldsymbol{y}$, the goal of this paper is to estimate the number of bands $M$ and the center frequency $f_j$ of each band. This task is complicated by the fact that Fourier analysis techniques, when applied to the finite vector of samples $\boldsymbol{y}$, are plagued by the problem of spectral leakage: the boundaries of the bands become smeared and bands can blend into one another.

### 1.2. Related Work

When all bands in the multiband signal have zero band width, our problem reduces to line spectral estimation [1, 12]. When the band widths are nonzero, however, those methods no longer apply. Most of the research involving the multiband signal model studies the signal sampling problem, in which the aim is to *reconstruct* the time domain multiband signal using a minimal sampling rate [10, 11, 13]. For example, [13] proposes periodic nonuniform sampling for mutiband signal reconstruction when the number of bands is known, [10] proposes a universal sampling pattern which requires the lowest and highest frequencies and the occupancy rate of the bands, and [11] studies sub-Nyquist sampling for spectrum-blind multiband signal recovery under a compressed sensing framework [14, 15]. More sampling schemes are available in [16, 17]. Meanwhile, [9] studies the multiband signal identification in the noiseless case, using discrete prolate spheroidal sequences (DPSS) [18] to construct a subspace model for the active bands and employing these in an atomic norm minimization framework [19, 20].

Deep learning has gained much attention in signal processing [8, 21] due to its efficiency and promising performance. Relevant to our work are [3, 4], which address line spectral estimation via

deep architectures for sample vectors of a fixed size. Their networks map the observed samples to a pseudo-spectrum [3], from which the frequencies can be located by finding peaks. This mapping process is inspired by atomic norm minimization methods [1, 9], which take time-domain samples and solve for the dual polynomial. In this paper, we extend these works to solve the multiband signal identification problem, and we allow for varying numbers of observed samples. Our work shows the potential to design deep architectures that enjoy both the efficiency of deep learning and the capability of leveraging extended data points for better performance. Specifically, we propose a novel multiband signal representation model, which combines a long short-term memory (LSTM) [22] and convolutional neural network [23], to encode the observed samples and map the encoded signal to a frequency spectrum representation. A counting model is then applied to estimate the number of bands, $M$, based on the predicted spectrum. The bands' centers can then be automatically extracted from the $M$ tallest peaks in the spectrum.

Our paper is organized as follows. In Section 2, we introduce the proposed multiband signal representation and counting models for multiband signal identification. Several numerical experiments are conducted in Section 3 to evaluate the effectiveness of the proposed method. We conclude this paper in Section 4.

## 2. PROPOSED METHOD

### 2.1. Multiband Signal Representation Model

For line spectral estimation, [3] demonstrates that predicting a frequency spectrum which encodes the frequency information is more effective than estimating the frequencies directly. Inspired by their methodology and traditional atomic norm optimization methods [1, 24], where a dual solution is constructed and a frequency spectrum can be plotted to locate the ground truth frequencies by correlating the dual solution against exponential atoms of different frequencies, our multiband signal representation model maps the observed signal to a *frequency spectrum* (FS) representation. In the dual polynomial-generated frequency spectrum, the ground truth frequencies would have magnitude 1 just like the estimated frequency spectrum in [3] and our work. An example of a length-50 observed signal, its length-1000 over-complete DFT, the signal's ground-truth bands, and the target frequency spectrum for the deep network are shown in Fig. 1. The target FS is a superposition of $M$ Gaussian kernels, $FS(f) = \sum_{j=1}^{M} K(f - f_j)$ where each Gaussian kernel has the form $K(f) = \exp(-f^2/\sigma_f^2)$. We set $\sigma_f = 0.006$ as in [4] and note that there is a trade-off between the resolution in the spectrum and the number of informative non-zero values for network calibration. The discretized FS is of length-1000 with circular periodization.

The architecture of the proposed multiband signal representation model, termed **DeepMultiband**, is shown in Fig. 2. The input of the model is $[\boldsymbol{y}_R, \boldsymbol{y}_I] \in \mathbf{R}^{N\times 2}$ where $\boldsymbol{y}_R$ and $\boldsymbol{y}_I$ denote the real and imaginary parts of the observed signal $\boldsymbol{y}$ and $\boldsymbol{y} = \boldsymbol{y}_R + i\boldsymbol{y}_I$. Long short-term memory (LSTM) [22] has achieved great success in handling data of different lengths and is introduced in our model to deal with varying length inputs ($N$ is not fixed). However, an individual exponential signal sample can not provide valuable information about the signal's frequency. Thus, we add an input convolutional layer, whose convolution kernel has the view of several consecutive data samples, to embed the raw time series exponential signal data. Intuitively, each embedded data point will contain the frequency and noise information within its time window. The LSTM is then responsible for examining all the embedded data and outputting a deconvolution signal. Specifically, an input convolution layer with kernel size 20 (we assume $N \geq 20$) first encodes the observed samples into a data bank of 30 channels, which results in an $(N-20+1)\times 30$ matrix. An LSTM with hidden size 200 then processes each row of the data matrix one at a time starting from the first row. After processing all encoded data, the last hidden state of size $200 \times 1$ is mapped to an intermediate feature space with 32 channels by a linear transformation. Intuitively, we expect that each feature channel encodes a Fourier transformation-like spectrum as in the network proposed in [4] for line spectral estimation. The transformed features are then processed by 20 convolutional neural network (CNN) blocks of the same structure but with different weights; the data preserves its size through those CNN blocks. Each CNN block consists of a convolution layer with kernel size 3 with circular padding to process the local frequency information, a batch norm minimization to facilitate the training, and a rectified linear unit (ReLU) layer to impose non-linearity. The structure of the CNN block in DeepMultiband and counting model in Section 2.2 are inspired by [3, 4] but with the hyper-parameters, e.g., the kernel size and number of feature channel, fine tuned based on the mutiband signals in our experiments. Finally, a transposed convolution layer [25] with kernel size 12 and stride 5 produces the estimated frequency spectrum of length 1000.

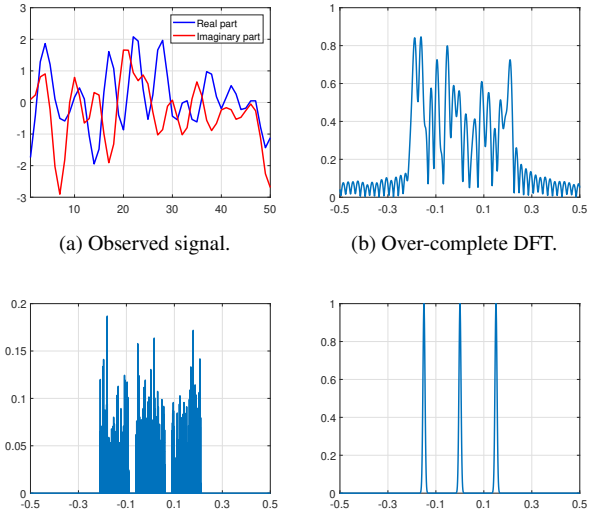


(a) Observed signal. (b) Over-complete DFT.

(c) Signal's ground-truth bands. (d) Target frequency spectrum.

**Fig. 1**: An observed signal of 50 length at SNR 30 dB, whose bands' digital frequency centers are $\{-0.15, 0, 0.15\}$ with digital band width $W = 3/N = 0.06$. (a) The real and imaginary parts of the observed signal. (b) The signal's 1000 length over-complete DFT. (c) The signal's ground-truth bands. (d) The target FS.

### 2.2. Multiband Signal Counting Model

Given the frequency spectrum estimated by a pre-trained DeepMultiband model, a counting model is trained to determine the number of bands within the observed signal. The input of the counting model is the estimated FS and the output is a single value that is rounded to the nearest integer. The counting model consists of an input convolution layer with 32 kernels of size 12 and stride 8, 20 CNN blocks as introduced in Section 2.1 with the same setting, an output convolution layer with kernel and output channel size 1, and a fully connected layer that outputs the final value.

978-1-7281-5767-2/21/$31.00 ©2021 IEEE

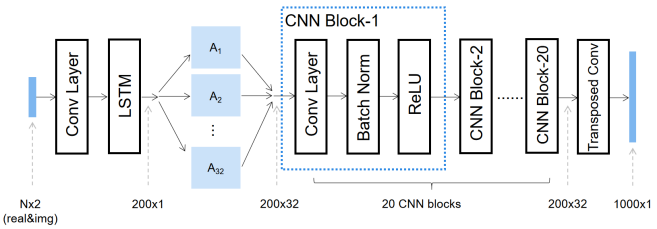


**Fig. 2**: DeepMultiband, the multiband signal representation model. The input and output sizes of the model and the data sizes between the hidden layers are marked below.

## 3. NUMERICAL EXPERIMENTS

### 3.1. Experiment Setup

We generate the simulation data based on (3). The training, validation, and testing data sets contain 200000, 1000, and 1000 multiband signals, respectively. The length of each multiband signal, $N$, is uniformly selected from $\{25, 26, \ldots, 50\}$, while the number of bands, $M$, is uniformly selected from $\{1, 2, 3\}$. The bands' digital frequency centers are uniformly sampled within $[-0.5, 0.5)$ with a minimal separation of $2W + 1/N$ so that they are not overlapping; we study the case of overlapping bands in Section 3.4. All bands have a fixed maximum digital band width $W = 0.06$ and 200 complex exponentials with frequencies uniformly sampled within $[f_j - W, f_j + W]$ are summed together to generate the corresponding signal component within the $j^{\text{th}}$ band. Each complex exponential's amplitude is generated as $(0.1 + |g|)e^{i\theta}$, where $g$ follows the standard normal distribution and $\theta$ is uniformly selected in $[0, 2\pi]$. We train the DeepMultiband and counting models for 200 and 100 epochs, respectively, with batch size 256 and using the Adam algorithm [26] with learning rate 0.001. In each epoch, we add additive Gaussian noise to the multiband signal to yield an SNR drawn from the uniform distribution over $[0, 50]$ dB. The loss functions for the DeepMultiband and counting models are the squared $\ell_2$ error between the ground-truth and predicted FS, $||FS_{gt} - FS_{pred}||_2^2$, and the squared error between the ground-truth number of bands and the predicted number of bands, $(M_{gt} - M_{pred})^2$, respectively. We train DeepMultiband first and the counting model second based on the FS predicted by a fixed-weight DeepMultiband.

**Compared methods.** Since the multiband signal identification problem can be viewed as a generalized line spectral estimation problem with a band convolution in the frequency domain, we implement the PSnet [3] and DeepFreq [4] models, which to the best of our knowledge are the state of the art deep architectures for line spectral estimation, for comparison. Because PSnet and DeepFreq take a fixed-length input, their networks are trained following the same setting as our model but using a truncated input consisting of the first 25 samples. In addition, for each compared deep model, a counting model is also trained based on its predicted FS to determine the number of bands. When the bands are modeled using the DPSS dictionary [18] in Section 3.5, we implement an atomic norm minimization method proposed in [9].

**Metrics.** We analyze the performance of the proposed method in terms of false negative rate (FNR), F1 score, and chamfer error. Specifically, FNR is defined as the percent of undetected true band centers. A successful detection is counted when there is a detected band center within $\pm 0.02$ of a true band center. The F1 score is calculated based on the precision and recall. The chamfer error [27] between the ground-truth bands' centers, $f_0 = \{f_1, \cdots, f_{n_1}\}$, and estimated centers, $\hat{f} = \{\hat{f}_1, \cdots, \hat{f}_{n_2}\}$, is $\frac{1}{n_1}\sum_{f_i \in f_0} \min_{\hat{f}_j \in \hat{f}} |f_i - \hat{f}_j| + \frac{1}{n_2}\sum_{\hat{f}_j \in \hat{f}} \min_{f_i \in f_0} |\hat{f}_j - f_i|$.

### 3.2. Effect Of The Signal Length

We first examine the capability of our model to handle different lengths of signals. The results with different SNRs are recorded in Fig. 3, where figures in the left column show different models' performance on the testing dataset with signal lengths following the uniform distribution over $[25, 50]$. Without retraining the models, figures in the right column of Fig. 3 present the models' performance with signal lengths uniformly drawn from $[100, 200]$. We observe that the DeepMultiband model outperforms other models at the low to middle SNRs when the signal length is within $[25, 50]$ and outperforms those models across all SNRs when the signal length is within $[100, 200]$. The results also show that the DeepMultiband model can leverage extended samples to achieve better performance. Note that when $N$ increases, the minimum separation $2W + 1/N$ reduces, which makes the identification problem harder. Taking a fixed-size input limits the problem complexity that PSnet and DeepFreq models can solve, which explains the diminished performance.

### 3.3. Effect Of The Band Shape

We again generate each signal in the testing dataset with length uniformly drawn from $[100, 200]$. For each band in the testing dataset, however, we evenly generate 200 exponentials within the band with magnitudes gradually increasing from 0.1 to 0.2. This gives all bands in the testing dataset a trapezoidal shape rather than the rectangular power spectrum used for training. Without retraining, the performance of different models on this testing dataset is recorded in Fig. 4. Although the performance of all models is slightly worse compared to the results in the right column of Fig. 3, our method still outperforms other models and achieves around 2% FNR, 0.98 F1 score, and 0.013 chamfer error when SNR is above 20 dB.

### 3.4. Multiband Signal With Overlapping Bands

To examine the effect of overlapping bands, we fix the number of bands in each multiband signal to 3, where the first and second bands have separation uniformly selected in $[W, 2W]$. Thus, there exist two bands with overlapping ratio uniformly drawn within $[0\%, 50\%]$ and another non-overlapping band that is at least $2W + 1/N$ separated from them. Since the number of bands is fixed, no counting model is needed. We retrain different representation models on this distribution with a signal length uniformly selected from $[25, 50]$. In Fig. 5, we record the performance of different models on the testing dataset with overlapping bands and signal length uniformly selected from $[100, 200]$. The results demonstrate that the DeepMultiband model is robust to the overlapping bands and outperforms other models by a large margin over the whole range of noise levels.

### 3.5. Multiband Signal Modeled By DPSS

The DPSS dictionary [18] gives a collection of time-limited and essentially band-limited functions. In this section, all bands in the training, validation, and testing datasets are generated using the DPSS dictionary of length 50 with $W = 3/N = 0.06$ and using the $2NW = 6$ most band-limited sequences. Dictionary coefficients follow the random normal distribution and are normalized to have unit $\ell_2$ norm. Thus, all observed samples have the same length of

978-1-7281-5767-2/21/$31.00 ©2021 IEEE

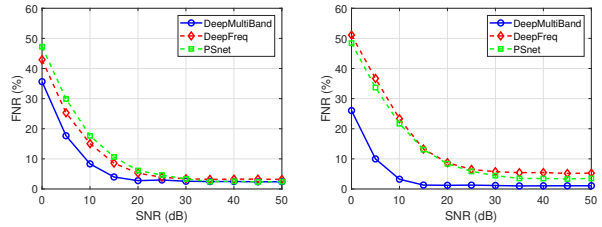


(a) False negative rate.




(b) False negative rate.

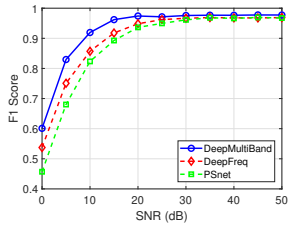


(c) F1 score.

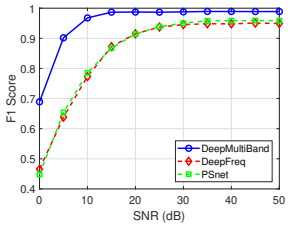


(d) F1 score.

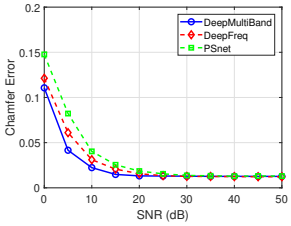


(e) Chamfer error.

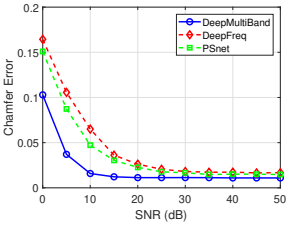


(f) Chamfer error.

**Fig. 3**: The effect of the length of the observed signal. Figures (a), (c), and (e) show the FNR, F1 score, and chamfer error of different models for signal lengths uniformly selected in $[25, 50]$. (b), (d), and (f) show the performance for signal lengths uniformly selected in $[100, 200]$ without retraining the models.

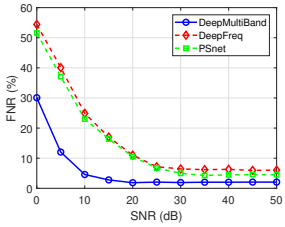


(a) False negative rate.

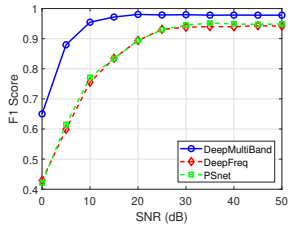


(b) F1 score.

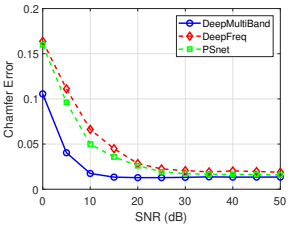


(c) Chamfer error.

**Fig. 4**: The effect of a nonrectangular power spectrum in each band.

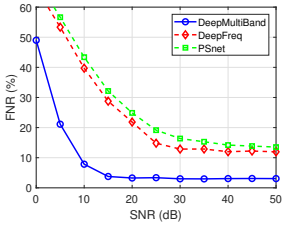


(a) False negative rate.

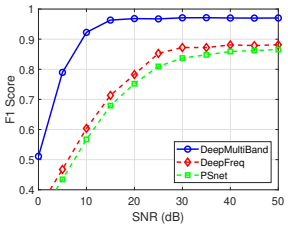


(b) F1 score.

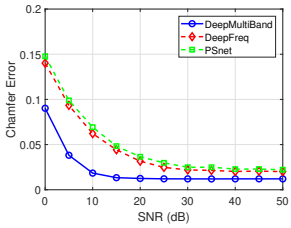


(c) Chamfer error.

**Fig. 5**: Multiband signal with overlapping bands.

50, and we retrain our DeepMultiband model on this distribution. The atomic norm minimization method proposed for multiband identification in [9] involves solving for a dual polynomial, but it does not include an estimator for the number of bands. Thus, the ground-truth number of bands is provided in this experiment. The performance of the atomic norm minimization method [9] and the proposed DeepMultiband method on noiseless mutiband signals are recorded in Table 1. Both methods perform very well in this case

**Table 1**: Noiseless multiband signal with bands modeled by DPSS.

| | FNR | F1 score | Chamfer error |
|---|---|---|---|
| AtomicNorm [9] | 0.15% | 0.9985 | 0.0009 |
| DeepMultiband | 0.07% | 0.9993 | 0.0012 |

and achieve less than $0.2\%$ FNR, over $0.99$ F1 score, and around $0.001$ chamfer error. It is worth noting, however, that our model is trained on the noisy dataset and thus is applicable to different noise levels, while [9] assumes a noiseless observation. Moreover, measured on an i7-6700 CPU, the DeepMultiband model only takes around $1.5$ seconds to predict the frequency spectrum for $1000$ multiband signals of length $50$, which is similar to DeepFreq and PSnet but more than two orders of magnitude faster than the atomic norm-based method [9] using CVX [28].

## 4. CONCLUSION

In this paper we solve the contaminated multiband signal identification problem via deep learning. A novel deep architecture, DeepMultiband, is proposed to map the observed varying-length multiband signal to a frequency spectrum; a counting model then determines the number of bands. Based on the estimated frequency spectrum and number of bands, the bands' centers can be identified automatically. Our experiments verify the effectiveness and robustness of the proposed method, which outperforms other state of the art deep architectures for line spectral estimation under a range of noise levels and is more than two orders of magnitude faster than atomic norm minimization.

978-1-7281-5767-2/21/$31.00 ©2021 IEEE

## 5. REFERENCES


[1] Badri Narayan Bhaskar, Gongguo Tang, and Benjamin Recht, "Atomic norm denoising with applications to line spectral estimation," *IEEE Transactions on Signal Processing*, vol. 61, no. 23, pp. 5987–5999, 2013.

[2] Zbigniew Leonowicz, Tadeusz Lobos, and Jacek Rezmer, "Advanced spectrum estimation methods for signal analysis in power electronics," *IEEE Transactions on Industrial Electronics*, vol. 50, no. 3, pp. 514–519, 2003.

[3] Gautier Izacard, Brett Bernstein, and Carlos Fernandez-Granda, "A learning-based framework for line-spectra super-resolution," in *ICASSP 2019-2019 IEEE International Conference on Acoustics, Speech and Signal Processing (ICASSP)*. IEEE, 2019, pp. 3632–3636.

[4] Gautier Izacard, Sreyas Mohan, and Carlos Fernandez-Granda, "Data-driven estimation of sinusoid frequencies," in *Advances in Neural Information Processing Systems*, 2019, pp. 5127–5137.

[5] Zhihui Zhu and Michael B Wakin, "On the dimensionality of wall and target return subspaces in through-the-wall radar imaging," in *2016 4th International Workshop on Compressed Sensing Theory and its Applications to Radar, Sonar and Remote Sensing (CoSeRa)*. IEEE, 2016, pp. 110–114.

[6] Michael Wakin, Stephen Becker, Eric Nakamura, Michael Grant, Emilio Sovero, Daniel Ching, Juhwan Yoo, Justin Romberg, Azita Emami-Neyestanak, and Emmanuel Candes, "A nonuniform sampler for wideband spectrally-sparse environments," *IEEE Journal on Emerging and Selected Topics in Circuits and Systems*, vol. 2, no. 3, pp. 516–529, 2012.

[7] Karol Gregor and Yann LeCun, "Learning fast approximations of sparse coding," in *Proceedings of the 27th international conference on international conference on machine learning*, 2010, pp. 399–406.

[8] Youye Xie, Zifan Wang, Weiping Pei, and Gongguo Tang, "Fast approximation of non-negative sparse recovery via deep learning," in *2019 IEEE International Conference on Image Processing (ICIP)*. IEEE, 2019, pp. 2921–2925.

[9] Zhihui Zhu, Dehui Yang, Michael B Wakin, and Gongguo Tang, "A super-resolution algorithm for multiband signal identification," in *2017 51st Asilomar Conference on Signals, Systems, and Computers*. IEEE, 2017, pp. 323–327.

[10] Ping Feng and Yoram Bresler, "Spectrum-blind minimum-rate sampling and reconstruction of multiband signals," in *1996 IEEE International Conference on Acoustics, Speech, and Signal Processing Conference (ICASSP)*. IEEE, 1996, vol. 3, pp. 1688–1691.

[11] Moshe Mishali and Yonina C Eldar, "Blind multiband signal reconstruction: Compressed sensing for analog signals," *IEEE Transactions on Signal Processing*, vol. 57, no. 3, pp. 993–1009, 2009.

[12] Zai Yang and Lihua Xie, "On gridless sparse methods for line spectral estimation from complete and incomplete data," *IEEE Transactions on Signal Processing*, vol. 63, no. 12, pp. 3139–3153, 2015.

[13] Yuan-Pei Lin, PP Vaidyanathan, et al., "Periodically nonuniform sampling of bandpass signals," *IEEE Transactions on Circuits and Systems Ii-Analog and Digital Signal Processing*, vol. 45, no. 3, pp. 340–351, 1998.

[14] Emmanuel J Candès and Michael B Wakin, "An introduction to compressive sampling," *IEEE signal processing magazine*, vol. 25, no. 2, pp. 21–30, 2008.

[15] Youye Xie, Michael B Wakin, and Gongguo Tang, "Support recovery for sparse signals with unknown non-stationary modulation," *IEEE Transactions on Signal Processing*, vol. 68, pp. 1884–1896, 2020.

[16] Mark A Davenport and Michael B Wakin, "Compressive sensing of analog signals using discrete prolate spheroidal sequences," *Applied and Computational Harmonic Analysis*, vol. 33, no. 3, pp. 438–472, 2012.

[17] Yijiu Zhao, Yu Hen Hu, and Jingjing Liu, "Random triggering-based sub-nyquist sampling system for sparse multiband signal," *IEEE Transactions on Instrumentation and Measurement*, vol. 66, no. 7, pp. 1789–1797, 2017.

[18] David Slepian, "Prolate spheroidal wave functions, fourier analysis, and uncertainty—v: The discrete case," *Bell System Technical Journal*, vol. 57, no. 5, pp. 1371–1430, 1978.

[19] Venkat Chandrasekaran, Benjamin Recht, Pablo A Parrilo, and Alan S Willsky, "The convex geometry of linear inverse problems," *Foundations of Computational mathematics*, vol. 12, no. 6, pp. 805–849, 2012.

[20] Youye Xie, Michael B Wakin, and Gongguo Tang, "Simultaneous sparse recovery and blind demodulation," *IEEE Transactions on Signal Processing*, vol. 67, no. 19, pp. 5184–5199, 2019.

[21] Yingheng Tang, Keisuke Kojima, Toshiaki Koike-Akino, Ye Wang, Pengxiang Wu, Youye Xie, Mohammad H Tahersima, Devesh K Jha, Kieran Parsons, and Minghao Qi, "Generative deep learning model for inverse design of integrated nanophotonic devices," *Laser & Photonics Reviews*, vol. 14, no. 12, pp. 2000287, 2020.

[22] Sepp Hochreiter and Jürgen Schmidhuber, "Long short-term memory," *Neural computation*, vol. 9, no. 8, pp. 1735–1780, 1997.

[23] Yann LeCun, Yoshua Bengio, and Geoffrey Hinton, "Deep learning," *nature*, vol. 521, no. 7553, pp. 436–444, 2015.

[24] Youye Xie, Shuang Li, Gongguo Tang, and Michael B Wakin, "Radar signal demixing via convex optimization," in *2017 22nd International Conference on Digital Signal Processing (DSP)*. IEEE, 2017, pp. 1–5.

[25] Hongyang Gao, Hao Yuan, Zhengyang Wang, and Shuiwang Ji, "Pixel transposed convolutional networks," *IEEE Transactions on Pattern Analysis and Machine Intelligence*, vol. 42, no. 5, pp. 1218–1227, 2019.

[26] Diederik P Kingma and Jimmy Ba, "Adam: A method for stochastic optimization," *arXiv preprint arXiv:1412.6980*, 2014.

[27] Youye Xie, Gongguo Tang, and William Hoff, "Chess piece recognition using oriented chamfer matching with a comparison to cnn," in *2018 IEEE Winter Conference on Applications of Computer Vision (WACV)*. IEEE, 2018, pp. 2001–2009.

[28] Michael Grant and Stephen Boyd, "CVX: Matlab software for disciplined convex programming, version 2.1," `http://cvxr.com/cvx`, Mar. 2014.